

000
001
002054
055
056003 **External Patch Group Prior Guided Internal Subspace Learning for Real Image
004 Denoising**057
058
059005
006
007060
061
062008
009
010063
064
065011
012
013066
067
068

014

069

015

070

Existing image denoising methods largely depends on noise modeling and estimation. The commonly used noise models, additive white Gaussian, are inflexible in describing the complex noise on real noisy images. This would limit the performance of existing methods on denoising real noisy images. In this paper, we firstly demonstrate that almost all state-of-the-art methods on removing Gaussian noise and real noise are limited in denoising real noisy images. We demonstrate that a simple Patch Group based Prior Learning model on RGB images can achieve better performance than existing denoising methods, especially the ones designed for real noise in natural images. Besides, we employ the external patch group prior learning for internal clustering and subspace learning. This external information guided internal denoising methods achieves even better than the external PG prior based methods and the fully internal PG prior based method. Through extensive on standard datasets on real noisy images with groundtruth, we demonstrate that the proposed method achieves much better denoising performance than the other state-of-the-art methods on Gaussian noise removal and real noise removal.

037
038071
072

039

073
074

040

075
076

041

077
078

042

079
080

043

081
082

044

083
084

045

085
086

046

087
088

047

089
090

048

091
092

049

093
094

050

095
096

051

097
098

052

099
100

053

101
102

Anonymous CVPR submission

Paper ID ****

Abstract

Therefore, the noise in real images are much more complex than Gaussian, and depends on camera series, brands, as well as the settings (ISO, shutter speed, and aperture, etc). The models designed to deal with AWGN would become much less effective on real noisy images.

In the last decade, the methods of [14, 15, 16, 17, 18, 19, 13] are designed to deal with real noisy images. Almost all these methods coincidentally employ a two-stage framework: in the first stage, assuming a distribution model (usually Gaussian) on the noise and estimate its parameters; in the second stage, performing denoising with the help of the noise modeling and estimation in the first stage. However, the Gaussian assumption is inflexible in describing the complex noise on real noisy images [16]. Although the mixture of Gaussians (MoG) model is possible to approximate any unknown noise [19], estimating its parameters is often time consuming via nonparametric Bayesian techniques [19, 20]. To evaluate the performance of these methods on dealing with complex real noise, we apply these methods, with corresponding default parameters, on a real noisy image provided in [13]. This image is captured by a Nikon D800 camera while the ISO is set as 3200. The "ground truth" image is also provided with which we can calculate objective measurements. More details about this dataset can be found at the experimental section. The denoised images are listed in Figure 1, from which we can see that these methods either remove the noise or oversmooth the complex details in real noisy image. This proves that the above mentioned methods are not effective on denoising complex noise on real images.

In this paper, we attempt to deal with complex noise in real images by integrating the external and internal information. Since the real noise is signal dependent [13, 23], the prior information in external natural images can be employed to avoid the high correlation between noise and signal in internal images. On the other hand, the internal prior is adaptive to the image and can recover better the latent clean image. Based on these observations, we make detailed study on internal and external information for real image denoising task. We made several observa-

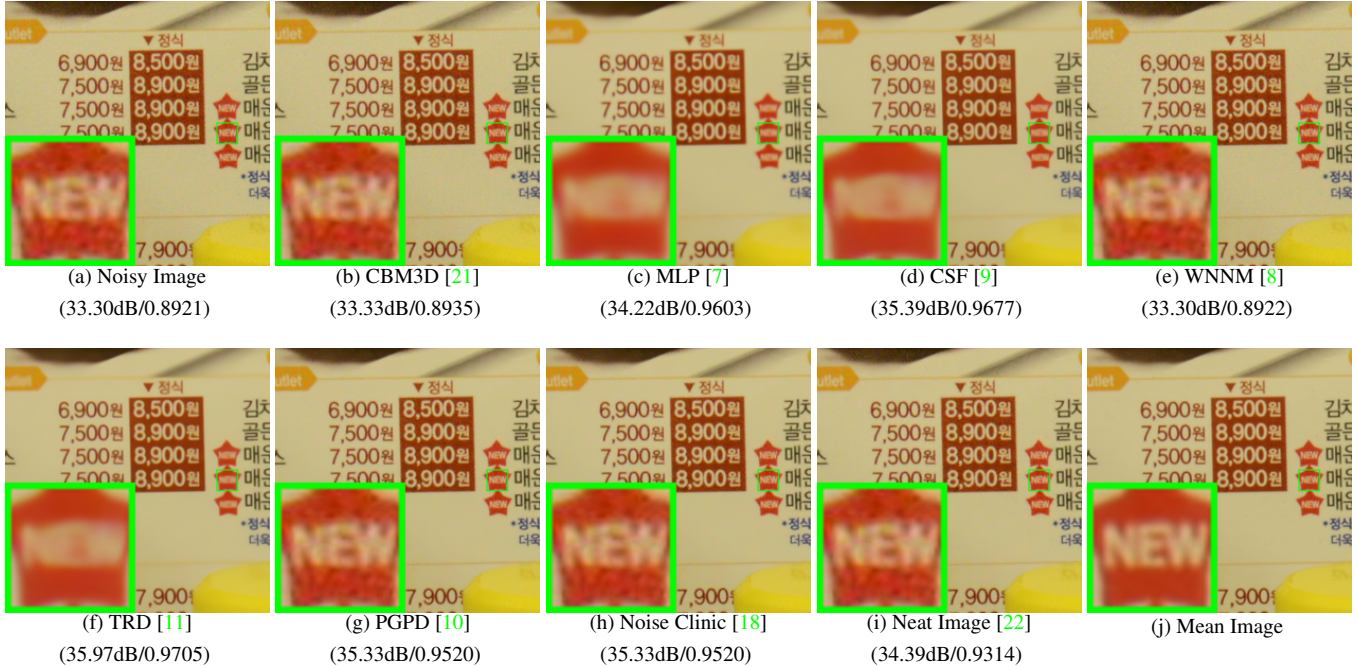


Figure 1. Denoised images of the real noisy image "NikonD800ISO3200A3" by different methods. The images are better to be zoomed in on screen.

tions. Firstly, we found that the Patch Group Prior learning based denoising method [10] learned on clean RGB images are enough to outperform the above mentioned denoising methods. Secondly, we also found that a fully internal PG prior based denoising method which achieve better performance than the fully external method. Most importantly, we found that the external PG prior guided internal method can achieve even better and faster performance on real image denoising. In fact, the external PG prior learning based model is employed to guide the clustering of internal PGs extracted from the input noisy images. Then for each cluster of PGs, we perform subspace learning by PCA and denoising by weighted sparse coding. We perform comprehensive experiments on real noisy images captured by different CMOS or CCS sensors. The results demonstrate that our method achieves comparable or even better performance on denoising real noisy images. This reveals the potential advantages of combining external and internal information of natural images on robust and complex real noisy image denoising problem.

1.1. Our Contributions

The contributions of this paper are summarized as follows:

- We propose a novel method which combine the external and internal PG prior for real noisy image denoising problem;
- Our method doesn't need noise modeling and estima-

tion, and the noise levels of real noisy images are automatically expressed by the singular values of learned subspace;

- We achieve much better performance on visual quality, PSNR, SSIM, and speed, than other competing methods for real image denoising problem.

The rest of this paper will be summarized as follows: in Section 2, we will introduce the related work close to our work; in Section 3, we will introduce our proposed external prior guided internal subspace learning framework for real image denoising; in Section 4, we will demonstrate the denoising experiments on several standard dataset; in Section 5, we will conclude our paper and give our future work.

2. Related Work

2.1. Patch Group Prior of Natural Images

Patch prior is an approximation of the prior of natural images. There are several famous work on this area such as the K-SVD algorithm [3]. The seminar work on patch prior modeling is the expected patch log likelihood (EPLL), which models the space of natural image patches via Gaussian Mixture Model. Recently, the Patch Group prior [10] is proposed to directly model the non-local self similarity within natural images. The patch group prior demonstrate better properties via better image denoising performance on natural images. However, PGPD only utilizes the information of clean natural images, but not fully make full

216 of the NSS information of noisy input images. In this pa-
 217 per, we combine the information of external natural clean
 218 images and internal real noisy images to achieve adaptive
 219 patch group prior modeling. In fact, we use the external
 220 Patch Group prior to guide the structural clustering of in-
 221 ternal patch groups in real noisy images. For each cluster
 222 of PGs, we propose to use PCA for subspace learning. The
 223 eigenvectors are the basis of this subspace and hence can be
 224 used as an orthonormal dictionary. The eigenvalues reflect
 225 the information describing the noise levels and hence can
 226 be used as parameters for image denoising. Noted that the
 227 dictionary and parameters are obtained via a fully unsuper-
 228 vised way by subspace learning. Therefore, our model is
 229 highly adaptive to the noisy input images.
 230

2.2. Internal v.s. External Image Denoising

231 The internal patch recurrence across multiple scales of a
 232 natural image has been successfully applied in many image
 233 restoration problems such as single image super-resolution
 234 [24], image denoising [25], blind image deblurring [26],
 235 and image dehazing [27], etc. These work demonstrate that
 236 internal information is enough for denoising additive white
 237 Gaussian noise. The reason is that the AWGN noise is in-
 238 dependent of the original clean images, and therefore it will
 239 be when the image is scaled to smaller size. However, the
 240 real noise is dependent on the signal [13] and it has fixed
 241 patterns from several main sources [23]. The internal infor-
 242 mation may be not enough for real image denoising prob-
 243 lem. Noted that even in denoising AWGN, the introduce of
 244 external information will also improve the performance de-
 245 noising methods [28]. In this paper, we demonstrate that for
 246 real noise which is signal dependent, it is essential to make
 247 use of external clean data.
 248

2.3. Real Image Denoising

249 To the best of our knowledge, the study of real image
 250 denoising can be dated back to the BLS-GSM model [29],
 251 in which Portilla et al. proposed to use scale mixture of
 252 Gaussian in overcomplete oriented pyramids to estimate the
 253 latent clean images. In [14], Portilla proposed to use a cor-
 254 related Gaussian model for noise estimation of each wavelet
 255 subband. Based on the robust statistics theory [?], the work
 256 of Rabie [15] modeled the noisy pixels as outliers, which
 257 could be removed via Lorentzian robust estimator. In [16],
 258 Liu et al. proposed to use ‘noise level function’ (NLF) to es-
 259 timate the noise and then use Gaussian conditional random
 260 field to obtain the latent clean image. Recently, Gong et al.
 261 proposed an optimization based method [17], which mod-
 262 els the data fitting term by weighted sum of ℓ_1 and ℓ_2 norms
 263 and the regularization term by sparsity prior in the wavelet
 264 transform domain. Later, Lebrun el al. proposed a multi-
 265 scale denoising algorithm called ‘Noise Clinic’ [18] for
 266 real image denoising task. This method generalizes the NL-

267 Bayes [30] to deal with signal, scale, and frequency depen-
 268 dent noise. Recently, Zhu et al. proposed a Bayesian model
 269 [19] which approximates the noise via Mixture of Gaussian
 270 (MoG) model [20]. The clean image is recovered from the
 271 noisy image by the proposed Low Rank MoG filter (LR-
 272 MoG). However, noise level estimation is already a chal-
 273 lenging problem and denoising methods are quite sensitive
 274 to this parameter. Moreover, these methods are based on
 275 shrinkage models that are too simple to reflect reality, which
 276 results in over-smoothing of important structures such as
 277 small-scale text and textures.
 278

3. External Patch Group Prior Guided Internal Subspace Learning

279 In this section, we formulate the framework of external
 280 Patch Group prior guided internal subspace learning. We
 281 first introduce the patch group prior leaning on clean natural
 282 RGB images. Then we formulate the external guided internal
 283 subspace learning. Finally, we discuss the differences
 284 between external subspaces and the corresponding internal
 285 subspace.
 286

3.1. External Patch Group Prior Learning on Clean Natural Images

287 Images often demonstrate highly nonlocal self-similarity
 288 (NSS) property, which refers to the fact that a patch always
 289 have similar patches to it around the image. This prop-
 290 erty is a key successful factor in image denoising methods
 291 [1, 4, 5, 31, 8] and restoration methods [?]. In [10], the
 292 NSS property is recently learned as an external prior in a
 293 patch group manner. In this section, we formulate the Patch
 294 Group prior on clean natural images.
 295

296 In external PG prior learning on clean natural images,
 297 a PG is obtained via finding the M most similar nonlocal
 298 patches to the local patch (size: $p \times p \times 3$ for RGB chan-
 299 nels) in a given clean image. The similarity is measured
 300 by Euclidean distance or other distance measurements. In
 301 this work, we find similar PGs through the Euclidean dis-
 302 tance based block matching in a large enough local window
 303 of size $W \times W$. The PG is denoted by $\{\mathbf{x}_m\}_{m=1}^M$, where
 304 $\mathbf{x}_m \in \mathbb{R}^{3p^2 \times 1}$ is a patch vector. The mean vector of this PG
 305 is $\mu = \frac{1}{M} \sum_{m=1}^M \mathbf{x}_m$, and $\bar{\mathbf{x}}_m = \mathbf{x}_m - \mu$ is the group mean
 306 subtracted patch vector. We call
 307

$$\bar{\mathbf{X}} \triangleq \{\bar{\mathbf{x}}_m\}, m = 1, \dots, M \quad (1)$$

308 the group mean subtracted PG, and it will be used to learn
 309 the NSS prior in our work. All these are similar with the
 310 definitions in [10].
 311

312 From a given set of natural images, we can extract N
 313 PGs, and PG as
 314

$$\bar{\mathbf{X}}_n \triangleq \{\bar{\mathbf{x}}_{n,m}\}_{m=1}^M, n = 1, \dots, N. \quad (2)$$

324 We employ the patch group based Gaussian Mixture Model
 325 (PG-GMM) for NSS prior learning. The learning process is
 326 the same with that in [10].
 327

328 With PG-GMM, we aim to learn a set of K Gaussians
 329 $\{\mathcal{N}(\mu_k, \Sigma_k)\}$ from N training PGs $\{\bar{\mathbf{X}}_n\}$, while requiring
 330 that all the M patches $\{\bar{\mathbf{x}}_{n,m}\}$ in PG $\bar{\mathbf{X}}_n$ belong to the same
 331 Gaussian component and assume that the patches in the PG
 332 are independently sampled. Note that such an assumption
 333 is commonly used in patch based image modeling [3, 5].
 334 Then, the likelihood of $\{\bar{\mathbf{X}}_n\}$ can be calculated as

$$335 P(\bar{\mathbf{X}}_n) = \sum_{k=1}^K \pi_k \prod_{m=1}^M \mathcal{N}(\bar{\mathbf{x}}_{n,m} | \mu_k, \Sigma_k). \quad (3)$$

337 By assuming that all the PGs are independently sampled,
 338 the overall objective log-likelihood function is
 339

$$340 \ln \mathcal{L} = \sum_{n=1}^N \ln \left(\sum_{k=1}^K \pi_k \prod_{m=1}^M \mathcal{N}(\bar{\mathbf{x}}_{n,m} | \mu_k, \Sigma_k) \right). \quad (4)$$

344 We maximize the above objective function for PG-GMM
 345 learning. Finally, we obtain the GMM model with three sets
 346 of parameters including mixture weights $\{\pi_k\}_{k=1}^K$, mean
 347 vectors $\{\mu_k = \mathbf{0}\}_{k=1}^K$, and covariance matrices $\{\Sigma_k\}_{k=1}^K$.
 348 Noted that in PGPD [10], the mean vector of each cluster is
 349 natural zeros, i.e., $\mu_k = \mathbf{0}$.

3.2. External PG Prior Guided Internal Subspace Learning

353 For each $\bar{\mathbf{Y}}$, we select the most suitable Gaussian com-
 354 ponent to it from the trained PG-GMM. Since the noise on
 355 real images are small when compared to the signals and the
 356 noise on real images are dependent on the signals, the covar-
 357 iance matrix of the k th component is still Σ_k . The selec-
 358 tion can be done by checking the posterior probability that
 359 $\bar{\mathbf{Y}}$ belongs to the k th Gaussian component:

$$361 P(k|\bar{\mathbf{Y}}) = \frac{\prod_{m=1}^M \mathcal{N}(\bar{\mathbf{y}}_m | \mathbf{0}, \Sigma_k)}{\sum_{l=1}^K \prod_{m=1}^M \mathcal{N}(\bar{\mathbf{y}}_m | \mathbf{0}, \Sigma_l)}. \quad (5)$$

364 Finally, the component with the highest probability
 365 $\ln P(k|\bar{\mathbf{Y}})$ is selected to process $\bar{\mathbf{Y}}$.

366 Suppose that the k th Gaussian component is selected for
 367 PG $\bar{\mathbf{Y}}$. For notation simplicity, we remove the subscript k
 368 and denote by Σ the covariance matrix of this component.
 369 In PG-GMM, the PGs actually represent the variations of
 370 the similar patches in a group, and these variations are as-
 371 signed to the same Gaussian distribution. By singular value
 372 decomposition (SVD), Σ can be factorized as

$$374 \Sigma = \mathbf{D} \Lambda \mathbf{D}^T, \quad (6)$$

376 where \mathbf{D} is an orthonormal matrix composed by the eigen-
 377 vectors of Σ and Λ is the diagonal matrix of eigenvalues.

378 With PG-GMM, the eigenvectors in \mathbf{D} capture the statis-
 379 tical structures of NSS variations in natural images, while
 380 the eigenvalues in Λ represent the significance of these
 381 eigenvectors. Fig. 4 shows the eigenvectors for 3 Gaus-
 382 sian components. It can be seen that these eigenvectors
 383 encode the possible variations of the PGs. For one Gaus-
 384 sian component, the first eigenvector represents its largest
 385 variation, while the last eigenvector represents its smallest
 386 variation. For different Gaussian components, we can see
 387 that their eigenvectors (with the same index) are very dif-
 388 ferent. Hence, \mathbf{D} can be used to represent the structural
 389 variations of the PGs in that component.

$$391 \min_{\alpha} \|\bar{\mathbf{y}}_m - \mathbf{D}\alpha\|_2^2 + \sum_{i=1}^{p^2} \frac{c}{\lambda_i} |\alpha_i|. \quad (7)$$

392 By comparing (7) with (??), we can see that the i th entry of
 393 the weighting vector \mathbf{w} should be

$$394 \mathbf{w}_i = c / (\lambda_i + \varepsilon), \quad (8)$$

395 where ε is a small positive number to avoid dividing by zero.
 396 With \mathbf{w} determined by (8), let's see what the solution of
 397 (??) should be. Since the dictionary \mathbf{D} is orthonormal, it
 398 is not difficult to find out that (??) has a closed-form solu-
 399 tion (detailed derivation can be found in the supplementary
 400 material):

$$401 \hat{\alpha} = \text{sgn}(\mathbf{D}^T \bar{\mathbf{y}}_m) \odot \max(|\mathbf{D}^T \bar{\mathbf{y}}_m| - \mathbf{w}/2, 0), \quad (9)$$

402 where $\text{sgn}(\bullet)$ is the sign function, \odot means element-wise
 403 multiplication, and $|\mathbf{D}^T \bar{\mathbf{y}}_m|$ is the absolute value of each
 404 entry of vector $|\mathbf{D}^T \bar{\mathbf{y}}_m|$. The closed-form solution makes
 405 our weighted sparse coding process very efficient.

3.3. What does External Data help the Internal Subspace Learning?

412 The external data can help the internal learning in two
 413 ways. On one hand, it can guide the noisy image patches to
 414 be divided into correct subspaces through clustering. If we
 415 cluster the noisy patches in an automatical way, just like the
 416 PLE [32] did, the signal dependent noise would be hardly
 417 removed. With the help of clean external data, the noisy
 418 patches can be divided into correct subspaces. Besides, ex-
 419 ternal data guided internal clustering is much more efficient
 420 than directly clustering the noisy data due to the time con-
 421 suming fitting procedure. On the other hand, due to the
 422 correct division of internal noisy data, the dictionary and
 423 pariters for subspace learning could be more adaptive to
 424 the testing real noisy image. Hence, it would achieve bet-
 425 ter denoising performance than the methods only using the
 426 external information.

3.4. The Internal PGs Spaces Are Subspaces of Corresponding External PG Spaces

428 In this subsection, we compare the distribution of exter-
 429 nal PGs extracted from clean natural images and real noisy

432 images. For better illumination, we randomly selected a
433 cluster and project the original clean PGs onto a 2-D plane.
434 Plot a Figure to demonstrate the data distributed in external
435 space and the assigned internal subspace. The internal sub-
436 space is only a subspace of the external space. Hence, if we
437 use the external data to perform denoising, the performance
438 would be limited due to the dependence of noise on signal.
439 If we combine the external and internal data for subspace
440 learning, the learned subspace would be too generative and
441 would therefore not specifically suitable for the testing data.
442

4. The Enhanced Algorithm

4.1. Iterative Regularization

443 Performig image denoising in one iteration is not
444 enough for real noise since the noise is signal dependent.
445 The removed noise in one iteration is largely dependent on
446 the signal. Therefore, it is essential to add back some resi-
447 duals removed in this iteration for the denoising of the next
448 iteration.

4.2. Effectively dealing with different noisy images

449 For real image denoising, we can perform well on images
450 which have similar noise levels with the training dataset.
451 How can we deal with the real noisy images whose noise
452 levels are higher than the training dataset? The answer is
453 to remove the noise by more iterations. The input image of
454 each iteration is the recovered image of previous iteration.
455 This makes sense since we can still view the recovered im-
456 age as a real noisy image.

457 This will also bring a second problem, that how we could
458 automatically terminate the iteration. This can be solved
459 by two methods. One way is to compare the images be-
460 tween two iterations and calculate their difference, the it-
461 eration can be terminated if the difference is smaller than
462 a threshold. The other way is to estimate the noise level
463 of the current image and terminate the iterations when the
464 noise level is lower than a preset threshold. We employ the
465 second way and set the threshold as 0.0001 in our ex-
466 periments. In fact, most of our testing images will be denoised
467 well in one iteration.

4.3. Efficient Model Selection by Gating Network

474 In the Gaussian component selection procedure, if we
475 employ the full posterior estimation, the speed is not fast.
476 Our algorithm can be speeded up by introducing the Gating
477 network model.

4.4. The Overall Algorithm

5. Experiments

484 In this section, we perform real image image denoising
485 experiments on three standard datasets. The first dataset is

486 real noisy images with mean images as ground truths pro-
487 vided by [13]. The second dataset is provided by the web-
488 site of Noise Clinic [18]. The third dataset is provided by
489 the Commercial software Neat Image [22]. The second and
490 third dataset do not have ground truth images.

5.1. Parameters Setting

491 The proposed method contains the PG prior learning
492 stage, the external prior guided internal subspace learning
493 stage, and the denoising stage. In the learning stage, simi-
494 lar to the PGPD, there are four parameters, p , M , W , and
495 K . We set $p = 6$ and hence the patch size is $6 \times 6 \times 3$.
496 The winodw size for searching PGs is $W = 31$. The num-
497 ber of similar patches is $N = 10$, the number of cluters is
498 set as $K = 33$. In the external prior guided learning stage,
499 there is no parameters. In the denoising stage, there are one
500 paramters, i.e., the λ which is used to regularize the sparse
501 term.

5.2. Comparison on External and Internal methods

502 In this subsection, we compared the proposed external
503 prior guided internal subspace learning model on real image
504 denoising. The three methods are evaluated on the dataset
505 provided in [13]. We calculate the PSNR, SSIM [?] and
506 visual quality of these three methods. We also compare the
507 speed. The PSNR and SSIM results on 60 cropped images
508 from [13] are listed in Table 1. The images are cropped into
509 size of 500×500 for better illustration. We also compare
510 the three methods on visual quality in Figure 5.2.

5.3. Comparison With other Competing Methods

511 We compare with previous state-of-the-art Gaussian
512 noise removal methods such as BM3D [4], WNNM [8],
513 MLP [7], CSF [9], and the recently proposed TRD [?]. We
514 also compare with three competing real image denoising
515 methods such as Noise Clinic, Neat Image, and the CC-
516 Noise method proposed recently. The popular software
517 NeatImage which is one of the best denoising software
518 available. All these methods need noise estimation which
519 is vary hard to perform if there is no uniform regions are
520 available in the testing image. The NeatImage will fail to
521 perform automatical parameters settings if there is no uni-
522 form regions.¹

5.4. Real Image Denoising

523 We the competing denoising methods from various re-
524 search directions on two datasets. Both the two datasets
525 comes from the [13]. The first dataset contains 17 images
526 of size over 7000×5000 . Since this dataset contains re-
527 currant contents across different images, we crop 60 small
528 images of size 500×500 from these 17 images in [13].

529 ¹To compare with CCNoise, we first transform the denoised images
530 into double format.



Figure 2. Denoised images of the old image "NikonD800ISO3200A3" by different methods. The images are better to be zoomed in on screen.

The PSNR and SSIM results are listed in table 2.

6. Conclusion and Future Work

In the future, we will evaluate the proposed method on other computer vision tasks such as single image super-resolution, photo-sketch synthesis, and cross-domain image recognition. Our proposed method can be improved if we use better training images, fine tune the parameters via cross-validation. We believe that our framework can be useful not just for real image denoising, but for image super-resolution, image cross-style synthesis, and recognition tasks. This will be our line of future work.

References

- [1] A. Buades, B. Coll, and J. M. Morel. A non-local algorithm for image denoising. *CVPR*, pages 60–65, 2005. 1, 3
- [2] S. Roth and M. J. Black. Fields of Experts. *International Journal of Computer Vision*, 82(2):205–229, 2009. 1
- [3] M. Elad and M. Aharon. Image denoising via sparse and redundant representations over learned dictionaries. *Image Processing, IEEE Transactions on*, 15(12):3736–3745, 2006. 1, 2, 4
- [4] K. Dabov, A. Foi, V. Katkovnik, and K. Egiazarian. Image denoising by sparse 3-D transform-domain collaborative filtering. *Image Processing, IEEE Transactions on*, 16(8):2080–2095, 2007. 1, 3, 5
- [5] J. Mairal, F. Bach, J. Ponce, G. Sapiro, and A. Zisserman. Non-local sparse models for image restoration. *ICCV*, pages 2272–2279, 2009. 1, 3, 4
- [6] D. Zoran and Y. Weiss. From learning models of natural image patches to whole image restoration. *ICCV*, pages 479–486, 2011. 1
- [7] Harold C Burger, Christian J Schuler, and Stefan Harmeling. Image denoising: Can plain neural networks compete with bm3d? *Computer Vision and Pattern Recognition (CVPR), 2012 IEEE Conference on*, pages 2392–2399, 2012. 1, 2, 5
- [8] S. Gu, L. Zhang, W. Zuo, and X. Feng. Weighted nuclear norm minimization with application to image denoising. *CVPR*, pages 2862–2869, 2014. 1, 2, 3, 5
- [9] U. Schmidt and S. Roth. Shrinkage fields for effective image restoration. *Computer Vision and Pattern Recognition (CVPR), 2014 IEEE Conference on*, pages 2774–2781, June 2014. 1, 2, 5
- [10] J. Xu, L. Zhang, W. Zuo, D. Zhang, and X. Feng. Patch group based nonlocal self-similarity prior learning for image denoising. *2015 IEEE International Conference on Computer Vision (ICCV)*, pages 244–252, 2015. 1, 2, 3, 4
- [11] Yunjin Chen, Wei Yu, and Thomas Pock. On learning optimized reaction diffusion processes for effective image restoration. *Proceedings of the IEEE Conference on Computer Vision and Pattern Recognition*, pages 5261–5269, 2015. 1, 2
- [12] S. J. Kim, H. T. Lin, Z. Lu, S. Ssstrunk, S. Lin, and M. S. Brown. A new in-camera imaging model for color computer vision and its application. *IEEE Transactions on Pattern Analysis and Machine Intelligence*, 34(12):2289–2302, Dec 2012. 1
- [13] Seonghyeon Nam, Youngbae Hwang, Yasuyuki Matsushita, and Seon Joo Kim. A holistic approach to cross-channel image noise modeling and its application to image denoising. *Proc. Computer Vision and Pattern Recognition (CVPR)*, pages 1683–1691, 2016. 1, 3, 5, 7
- [14] J. Portilla. Full blind denoising through noise covariance estimation using gaussian scale mixtures in the wavelet domain. *Image Processing, 2004. ICIP '04. 2004 International Conference on*, 2:1217–1220, 2004. 1, 3
- [15] Tamer Rabie. Robust estimation approach for blind denoising. *Image Processing, IEEE Transactions on*, 14(11):1755–1765, 2005. 1, 3
- [16] C. Liu, R. Szeliski, S. Bing Kang, C. L. Zitnick, and W. T. Freeman. Automatic estimation and removal of noise from a single image. *IEEE Transactions on Pattern Analysis and Machine Intelligence*, 30(2):299–314, 2008. 1, 3
- [17] Zheng Gong, Zuowei Shen, and Kim-Chuan Toh. Image restoration with mixed or unknown noises. *Multiscale Modeling & Simulation*, 12(2):458–487, 2014. 1, 3
- [18] M. Lebrun, M. Colom, and J.-M. Morel. Multiscale image blind denoising. *Image Processing, IEEE Transactions on*, 24(10):3149–3161, 2015. 1, 2, 3, 5

648

Table 1. Average PSNR(dB) results of different methods on 60 cropped real noisy images captured in [13].

702

649

Image	Noisy	CBM3D	WNNM	MLP	CSF	TRD	NI	NC	Offline	Online	Guided
PSNR	34.51	34.58	34.52	36.19	37.40	37.75	36.53	37.57	38.19	38.07	38.46
SSIM	0.8718	0.8748	0.8743	0.9470	0.9598	0.9617	0.9241	0.9514	0.9663	0.9625	0.9677

703

650

704

651

705

652

706

653

707

654

708

Table 2. Average PSNR(dB) results of different methods on 15 cropped real noisy images used in [13].

709

655

710

656

711

657

712

658

713

659

714

660

- [19] Fengyuan Zhu, Guangyong Chen, and Pheng-Ann Heng. From noise modeling to blind image denoising. *The IEEE Conference on Computer Vision and Pattern Recognition (CVPR)*, June 2016. 1, 3
- [20] C. M. Bishop. *Pattern recognition and machine learning*. New York: Springer, 2006. 1, 3
- [21] K. Dabov, A. Foi, V. Katkovnik, and K. Egiazarian. Color image denoising via sparse 3d collaborative filtering with grouping constraint in luminance-chrominance space. *IEEE International Conference on Image Processing*, 1, 2007. 2
- [22] Neatlab ABSoft. Neat image. <https://ni.neatvideo.com/home>. 2, 5
- [23] Glenn E Healey and Raghava Kondapudy. Radiometric ccd camera calibration and noise estimation. *IEEE Transactions on Pattern Analysis and Machine Intelligence*, 16(3):267–276, 1994. 1, 3
- [24] Daniel Glasner, Shai Bagon, and Michal Irani. Super-resolution from a single image. *ICCV*, 2009. 3
- [25] Maria Zontak, Inbar Mosseri, and Michal Irani. Separating signal from noise using patch recurrence across scales. *Proceedings of the IEEE Conference on Computer Vision and Pattern Recognition*, pages 1195–1202, 2013. 3
- [26] Tomer Michaeli and Michal Irani. Blind deblurring using internal patch recurrence. *European Conference on Computer Vision*, pages 783–798, 2014. 3
- [27] Y. Bahat and M. Irani. Blind dehazing using internal patch recurrence. *IEEE International Conference on Computational Photography (ICCP)*, pages 1–9, May 2016. 3
- [28] Enming Luo, Stanley H Chan, and Truong Q Nguyen. Adaptive image denoising by targeted databases. *IEEE Transactions on Image Processing*, 24(7):2167–2181, 2015. 3
- [29] J. Portilla, V. Strela, M.J. Wainwright, and E.P. Simoncelli. Image denoising using scale mixtures of Gaussians in the wavelet domain. *Image Processing, IEEE Transactions on*, 12(11):1338–1351, 2003. 3
- [30] M. Lebrun, A. Buades, and J. M. Morel. A nonlocal bayesian image denoising algorithm. *SIAM Journal on Imaging Sciences*, 6(3):1665–1688, 2013. 3
- [31] W. Dong, L. Zhang, G. Shi, and X. Li. Nonlocally centralized sparse representation for image restoration. *Image Processing, IEEE Transactions on*, 22(4):1620–1630, 2013. 3

- [32] G. Yu, G. Sapiro, and S. Mallat. Solving inverse problems with piecewise linear estimators: From Gaussian mixture models to structured sparsity. *Image Processing, IEEE Transactions on*, 21(5):2481–2499, 2012. 4

715

716

717

718

719

720

721

722

723

724

725

726

727

728

729

730

731

732

733

734

735

736

737

738

739

740

741

742

743

744

745

746

747

748

749

750

751

752

753

754

755

756

757

758

759

760

761

762

763

764

765

766

767

768

769

770

771

772

773

774

775

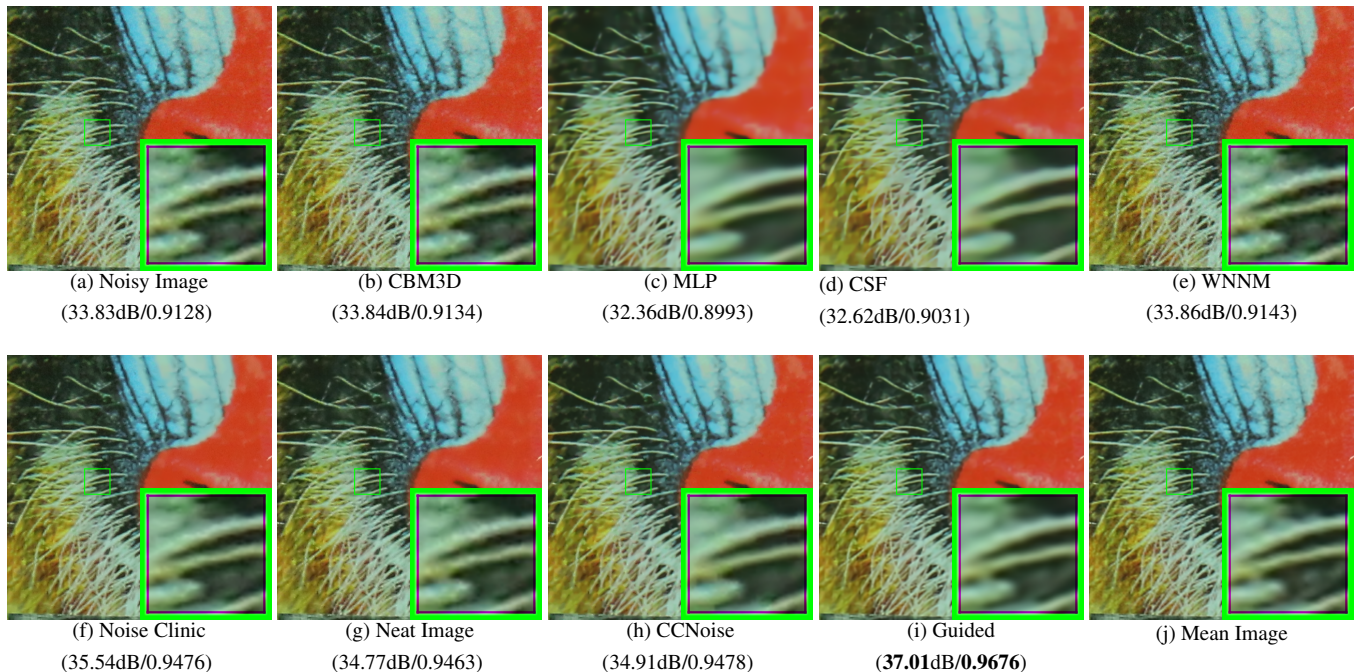
776

777

778

779

Figure 3.



810

811

812

813

814

815

816

817

818

819

820

821

822

823

824

825

826

827

828

829

830

831

832

833

834

835

836

837

838

839

840

841

842

843

844

845

846

847

848

849

850

851

852

853

854

855

856

857

858

859

860

780

781

782

783

784

785

786

787

788

789

790

791

792

793

794

795

796

797

798

799

800

801

802

803

804

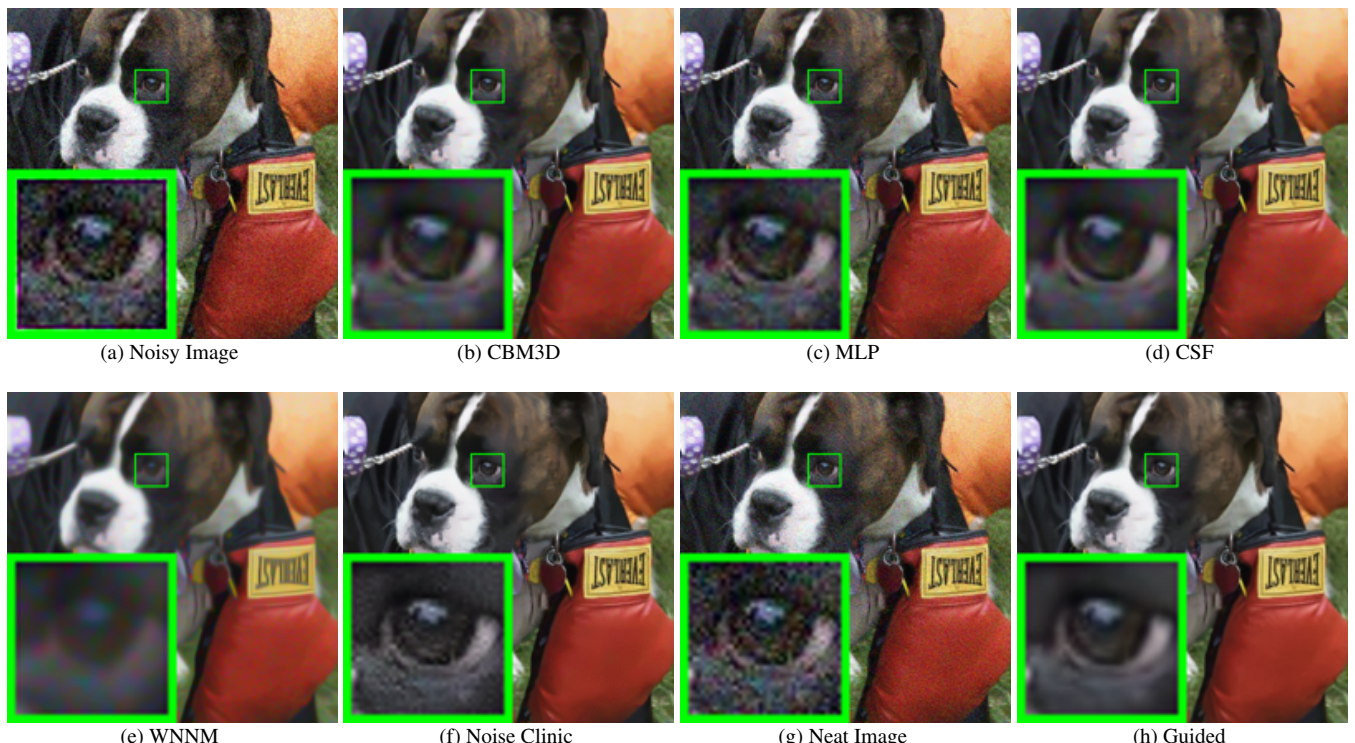
805

806

807

808

809



857

858

859

860

861

862

863

Figure 4. Denoised images of the old image "5dmark3iso32003" by different methods. The images are better to be zoomed in on screen.